

Remote Control of T Cell Activation Using Magnetic Janus Particles

Kwahun Lee, Yi Yi, and Yan Yu*

Abstract: We report a strategy for using magnetic Janus microparticles to control the stimulation of T cell signaling with single-cell precision. To achieve this, we designed Janus particles that are magnetically responsive on one hemisphere and stimulatory to T cells on the other side. By manipulating the rotation and locomotion of Janus particles under an external magnetic field, we could control the orientation of the particle–cell recognition and thereby the initiation of T cell activation. This study demonstrates a step towards employing anisotropic material properties of Janus particles to control single-cell activities without the need of complex magnetic manipulation devices.

Cells sense their environment and signal one another through receptor–ligand recognition. The binding of ligands to specialized cell surface receptors activates intracellular signaling pathways that determine the behavior of cells. Our ability to regulate these signaling events is essential for not only fundamental understanding of cell biology, but also engineering of cell functions for treating diseases.^[1] Among the various strategies for controlling cell signaling with external stimuli, magnetic manipulation is widely used owing to its unique advantages, such as the precise control over the intensity and direction of magnetic forces as well as minimal damage to living cells, in comparison to optical techniques.^[1a,2] Rotating magnetic fields have been used to twist magnetic nanoparticles to control the opening of ion channels,^[3] measure the mechanical properties of the cell cytoplasm and cytoskeleton,^[4] and probe the mechanotransduction of cell surface receptors.^[5] Local heating of magnetic nanoparticles has also been exploited to activate temperature-sensitive ion channels in neuron cells.^[1a] Several groups have used the aggregation of magnetic nanoparticles as a switch to activate cell signaling.^[2a–c,6] In those studies, magnetic nanoparticles were coated with ligands specific for a target signaling pathway,^[2a,c,6a,b] such as the apoptosis of tumor cells^[6d] or immune cell stimulation.^[2b,6c] When nanoparticles aggregated under the influence of a magnetic field, they induced the clustering of the membrane receptors to which they were bound and triggered the desired cell responses. A similar strategy has also been used with nanoparticles inside cells to regulate the nucleation and assembly of cytoskeletal proteins.^[7] However, these methods do not allow control of signaling with single-cell precision because the aggregation of magnetic nanoparticles cannot be con-

trolled locally unless a complex apparatus, such as a magnetic tweezer, is used to generate localized magnetic fields.^[8]

Herein, we present a strategy that employs magnetic Janus microparticles to remotely control the stimulation of single T cells with only hand-held magnets. T cell activation is a critical step in cancer immunotherapy, in which a cancer patient's own T cells are stimulated, either in vivo or in vitro, to recognize and attack cancer cells.^[9] Being able to remotely control which T cells to stimulate and switch the cell response on and off is an attractive strategy for the precise administration of the cancer therapy, but it remains a grand challenge. In this study, we achieved the remote control of activation of single T cells by exploiting the unique magnetic response of Janus particles. In our experimental design, one side of these particles was coated with a thin film of magnetically responsive materials, so that their orientation and locomotion can be controlled simultaneously. The Janus particles are also biologically anisotropic in that they display stimulatory ligand only on one hemisphere for T cell activation. In this way, we could control the initiation of T cell activation by manipulating the timing and the orientation of particle–cell contacts.

The 3 μm Janus particles were rendered magnetically responsive by applying a thin nickel coating on one hemisphere. Using thermal evaporation deposition, we sequentially deposited 50 nm of nickel and 30 nm of aluminum onto one hemisphere of monodisperse silica microparticles (Supporting Information, Figure S1). The thickness of the nickel coating was chosen to produce a robust magnetic response of particles while minimizing particle aggregation. The aluminum coating was used as a protective layer to keep the nickel film from oxidation. The silica hemisphere was functionalized with anti-CD3 antibody through streptavidin–biotin linkers. Anti-CD3 binds to the T cell receptor complexes on the cell surface and triggers T cell activation. The exposed surface of particles was passivated with bovine serum albumin (BSA) proteins, which prevents non-specific protein adsorption but induces no T cell responses.

We first set out to control the motion of Janus particles by rotating a permanent magnet near the imaging chamber (Figure S2a). The magnetic field was rotated around the x -, y -, or z -axis with respect to the imaging plane (also the bottom of the imaging chamber). We observed that Janus particles aligned with their Janus interface (the boundary between the two differently coated hemispheres of the particle) parallel to the external magnetic field and perpendicular to the imaging plane; they also rotated in the same direction as the rotating magnetic field (Figure 1a and S2). This agrees with previous studies, which have shown that a Janus particle with a thin nickel cap has a net magnetic dipole that is parallel to the Janus interface.^[10] This magnetic dipole is also shifted away from the geometric center of the particle.^[11] Owing to this

[*] K. Lee, Dr. Y. Yi, Prof. Y. Yu
Department of Chemistry, Indiana University
800 E. Kirkwood Ave., Bloomington, IN 47405 (USA)
E-mail: yy33@indiana.edu

Supporting information for this article can be found under:
<http://dx.doi.org/10.1002/anie.201601211>.

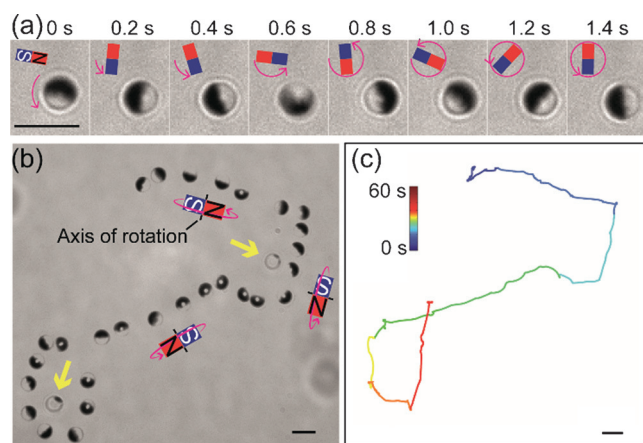


Figure 1. Remote control of the rotation and locomotion of magnetic Janus spheres. a) Snapshots showing the rotation of a single Janus sphere under a magnetic field that was rotated counterclockwise. b) Superimposed bright-field images showing that rotation and locomotion of a single Janus sphere can be simultaneously controlled to circumvent stationary particles (indicated by the yellow arrows) that were not magnetic responsive. c) Trajectory of the Janus sphere shown in (b). Scale bars = 5 μm .

shifted dipole effect, Janus particles moved translationally when they were rotated around the axis perpendicular to the Janus interface, and the direction of their locomotion was determined by the direction of the rotation (Figures 1 b,c and S2c). In other words, rotating the magnetic field around the z -axis changed the orientation of the Janus particles, but caused no locomotion. Rotating the magnetic field around the x - or y -axis induced the locomotion of particles without changing their orientation. By combining these different magnetic responses of Janus particles, we were able to simultaneously control the orientation and locomotion of the Janus particles. The rotational and translational speeds of Janus particles were controlled up to $15.7 \text{ rad sec}^{-1}$ and $7.0 \mu\text{m sec}^{-1}$, respectively, under a magnetic field of $\approx 14.2 \text{ mT}$.

We next sought to manipulate the triggering of T cell activation by magnetically controlling the Janus particles. Given that the stimulatory ligand, anti-CD3, is functionalized on only one side of our Janus particles, we hypothesized that the triggering of T cell activation could be controlled by manipulating the timing of the initial contact between T cells and the anti-CD3-coated hemisphere of the particles (Figure 2a). We quantified T cell activation by measuring the concentration fluctuation of intracellular Ca^{2+} ions. T cell activation is accompanied by the sudden influx of Ca^{2+} into the cell cytosol from both the endoplasmic reticulum (ER) and the extracellular environment.^[12] More intense and persistent calcium elevations indicate stronger T cell activation. In our experiments, the influx of Ca^{2+} was reported by a calcium sensitive dye, Fluo-4, which was loaded into the cell cytosol. The fluorescence emission of Fluo-4 increases proportionally to intracellular $[\text{Ca}^{2+}]$, so it provides a direct and quantitative readout of the T cell activation. As shown in Figure 2b, resting T cells containing Fluo-4 exhibited only weak fluorescence. A Janus particle that was coated with anti-CD3 on one hemisphere was moved using the rotating magnetic field to make contact with the cell from its metal-coated hemisphere. It was then rotated so that its anti-CD3 coated side faced the cell. A rapid increase of Fluo-4 fluorescence intensity was observed following the binding of the anti-CD3 side of the particle to the cell, and the fluorescent signal persisted for over a minute before gradually decreasing to the base level (Figure 2c). This time-dependent fluctuation of $[\text{Ca}^{2+}]$ indicated T cell activation. We chose which individual cell to stimulate by controlling the lateral trajectory of the Janus particles. We observed that once the anti-CD3 side bound to the cell surface, the magnetic control was not strong enough to further rotate the particles.

To further demonstrate that the timing of T cell activation was controlled by the orientation of Janus particles, we varied the time at which the anti-CD3 side of the particle was rotated to face the cell over a range of 0 to 180 seconds. For simplicity, the interval between when the metal-coated side of a particle contacted a T cell and when the anti-CD3 side was rotated to

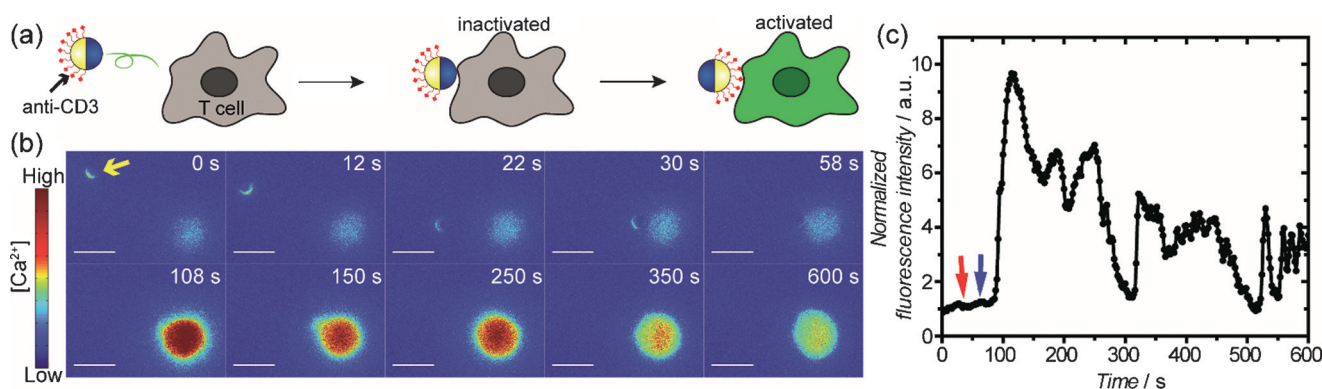


Figure 2. Remote control of T cell activation by controlling the rotation and locomotion of Janus particles. a) Illustration showing the orientation of a Janus sphere and the corresponding T cell response. b) Fluorescence images showing T cell activation when the anti-CD3 coated hemisphere of a Janus sphere (indicated by the yellow arrow) was rotated to face the cell. Images are color-coded based on fluorescence intensity of the calcium reporter Fluo-4. c) The normalized fluorescence intensity of the T cell shown in (b) is plotted against time to show the time dependence of T cell activation. The red arrow indicates the time when the metal-coated hemisphere made contact with the T cell and the blue arrow indicates the time when the anti-CD3 side was rotated to face the cell. Results are representative of $N = 51$ cells. Scale bars = 10 μm .

face the cell is referred to as the “rotation timing”. In the calcium plots of individual cells, we observed that the calcium elevation peak, which indicates the initiation of T cell activation, exhibited a delay corresponding to the rotation timing (Figure 3a). This correspondence is evident in the

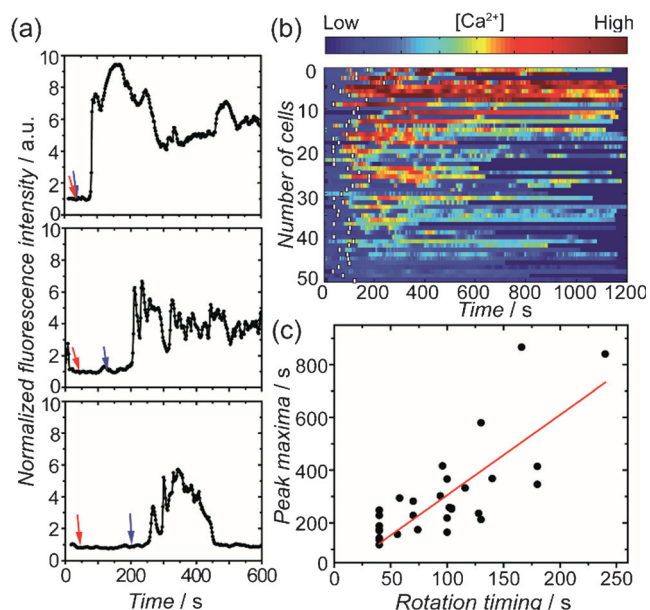


Figure 3. Manipulation of the initiation of T cell activation. a) Plots showing the calcium response of three representative cells as a function of time. In all plots, red arrows indicate the time when the metal-coated hemisphere made contact with T cells and blue arrows indicate the time when the anti-CD3 coated hemisphere was rotated to face the cells. b) Color-scaled heat map showing calcium response of T cells ($N=51$). White bars indicate the time when the anti-CD3-coated hemispheres were rotated to face the T cells. c) A plot showing the time of the calcium peak as a function of the rotation timing, which is defined as the time from when the metal side of a particle faced a T cell to when the anti-CD3 coated side was rotated to face the cell. Pearson's coefficient = 0.76.

calcium influx heat map, in which the calcium response of a large group of T cells ($N=51$) is color-coded based on the Fluo-4 intensity (Figure 3b). We noticed that a small fraction of cells showed calcium influx before the anti-CD3 hemisphere of particles was rotated to face them. The most probable cause of this is that the ruffling cell membrane may have occasionally made contact with the anti-CD3 hemisphere even when that side was facing away. We performed two sets of control experiments, in which Janus particles were either coated with the IgG2a isotype control of the anti-CD3 antibody or passivated with BSA only (Figure S3). Minimal T cell calcium response was observed in both control experiments, confirming that the T cell activation is specifically triggered by the anti-CD3 coated hemisphere. To quantify the correlation between the timing of T cell response and the orientation of particles, we plotted the time when each cell exhibited the calcium peak against the respective rotation timing (Figure 3c). The Pearson's coefficient was 0.76, indicating that prolonged rotation timing clearly delays calcium response in T cells. These results demonstrated our

capability to manipulate the initiation of T cell activation by controlling the rotation and locomotion of the Janus particles.

We next explored the remote control of T cell activation by rod-shaped Janus particles to test the generality of our approach. To prepare Janus rods, we first synthesized silica rods $0.83 \pm 0.07 \mu\text{m}$ in diameter and $2.56 \pm 0.17 \mu\text{m}$ in length. The silica rods were further coated on one hemicylinder with 50 nm of nickel and 30 nm of aluminum sequentially (Figure S4). The larger dimension of the nickel film along the long axis than that across the rod diameter gives rise to a net magnetic dipole parallel to the long axis. As demonstrated in Figures 4a and S5, the Janus rods could be rotated both in-

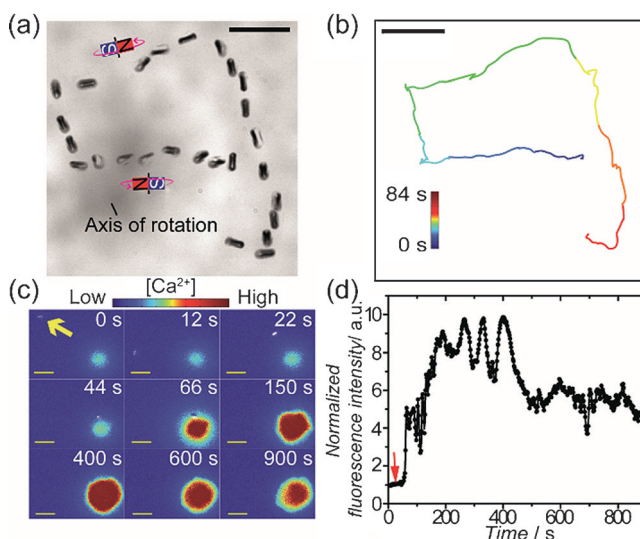


Figure 4. Remote control of T cell activation using magnetic Janus rods. a) Superimposed bright-field images showing the magnetic control of the rotation and locomotion of a Janus rod. b) Trajectory of the Janus rod shown in (a). c) Fluorescence images showing T cell activation by a rotating Janus rod (indicated by the yellow arrow). Images are color-coded based on the fluorescence intensity of the calcium reporter Fluo-4 in cells. d) The normalized fluorescence intensity of the T cell shown in (c) is plotted against time to show the time dependence of the T cell activation. Red arrow indicates the time when the Janus rod was rotated to make initial contact with the T cell. The results are representative of $N=18$ cells. Scale bars = $10 \mu\text{m}$.

plane and out-of-plane (tumbling) by varying the orientation of the external magnetic field. The out-of-plane rotation of the rods also led to translational displacement. The remote control of T cell activation was performed using a procedure similar to that was used for Janus spheres. A rapid increase in Fluo-4 fluorescence intensity, which indicates the onset of T cell activation, was observed when Janus rods were moved to make contact with the cell (Figure 4c,d). However, owing to the small diameter of the Janus rods and the fact that only one hemicylinder was visible in the fluorescence images, we could not determine which side of the Janus rods made contact with the cells.

This study demonstrates the first step in employing magnetic Janus particles as remote switches for controlling T cell signaling. In our study, one side of each Janus particle was magnetically responsive, while the other side displayed

ligands for triggering T cell activation. By simultaneously controlling the rotation and locomotion of the Janus particles, we regulated the initiation of T cell activation with single-cell precision. This spatiotemporal control was achieved by using simple hand-held magnets, in contrast to studies that relied on the use of magnetic tweezers for localized control of individual cells.^[8] We also demonstrate the generality of this approach by using Janus rods. Our group has shown previously that the anisotropic presentation of ligands on Janus particles changes the strength of T cell activation.^[13] But a limitation from that study was the lack of control over the orientation of particles for better interaction with cells. This study provides a step to overcome that limitation. In future studies, it will be important to establish the quantitative relationship between the cell response and the surface presentation of anti-CD3 on the Janus particles, as studies have shown that the strength of T cell activation depends on both the density and the amount of the stimulatory ligands.^[14] We will also combine the unique magnetic response and anisotropic surface functionality of Janus particles to enable the simultaneous control of multiple cell signaling pathways. This study showcases a potentially useful tool for the precise control of T cell activation in cancer immunotherapy.

Acknowledgements

We thank Dr. Stephen Anthony (Sandia National Laboratories) for the Matlab script of calcium imaging analysis, Dr. Jim Powers at the IUB Light Microscopy Imaging Center for assistance with imaging, and Indiana University for funding. This project was supported in part by the Indiana Clinical and Translational Sciences Institute, funded in part by grant #UL1 TR001108 from the National Institutes of Health, National Center for Advancing Translational Sciences, Clinical and Translational Sciences Award. Particle fabrication and characterization were carried out in the Nanoscale Characterization Facility at Indiana University.

Keywords: colloids · immunology · Janus particles · magnetic properties · nanotechnology

How to cite: *Angew. Chem. Int. Ed.* **2016**, *55*, 7384–7387
Angew. Chem. **2016**, *128*, 7510–7513

- [1] a) H. Huang, S. Delikanli, H. Zeng, D. M. Ferkey, A. Pralle, *Nat. Nanotechnol.* **2010**, *5*, 602–606; b) S. Wang, S. Szobota, Y. Wang, M. Volgraf, Z. Liu, C. Sun, D. Trauner, E. Y. Isacoff, X. Zhang, *Nano Lett.* **2007**, *7*, 3859–3863; c) C. I. De Zeeuw, F. E. Hoe-

- beek, L. W. J. Bosman, M. Schonewille, L. Witter, S. K. Koekoek, *Nat. Rev. Neurosci.* **2011**, *12*, 327–344; d) A. D. Luster, R. Alon, U. H. von Andrian, *Nat. Immunol.* **2005**, *6*, 1182–1190.
[2] a) E. M. Zhang, M. F. Kircher, M. Koch, L. Eliasson, S. N. Goldberg, E. Renstrom, *ACS Nano* **2014**, *8*, 3192–3201; b) K. Perica, A. Tu, A. Richter, J. G. Bieler, M. Edidin, J. P. Schneck, *ACS Nano* **2014**, *8*, 2252–2260; c) D. Kilinc, A. Lesniak, S. A. Rashdan, D. Gandhi, A. Blasiak, P. C. Fannin, A. von Kriegsheim, W. Kolch, G. U. Lee, *Adv. Healthcare Mater.* **2015**, *4*, 395–404; d) J. Dobson, *Nat. Nanotechnol.* **2008**, *3*, 139–143; e) L. Bonnemay, C. Hoffmann, Z. Gueroui, *WIREs Nanomed. Nanobiotechnol.* **2015**, *7*, 342–354; f) S. M. Lee, H. J. Kim, Y. J. Ha, Y. N. Park, S. K. Lee, Y. B. Park, K. H. Yoo, *ACS Nano* **2013**, *7*, 50–57; g) H. Kress, J. G. Park, C. O. Mejean, J. D. Forster, J. Park, S. S. Walse, Y. Zhang, D. Q. Wu, O. D. Weiner, T. M. Fahmy, E. R. Dufresne, *Nat. Methods* **2009**, *6*, 905–909; h) B. Moser, P. Loetscher, *Nat. Immunol.* **2001**, *2*, 123–128.
[3] S. Hughes, S. McBain, J. Dobson, A. J. El Haj, *J. R. Soc. Interface* **2008**, *5*, 855–863.
[4] a) J. F. Berret, *Nat. Commun.* **2016**, *7*, 10134; b) W. Möller, S. Takenaka, M. Rust, W. Stahlhofen, J. Heyder, *J. Aerosol Med.* **1997**, *10*, 173–186.
[5] N. Wang, J. P. Butler, D. E. Ingber, *Science* **1993**, *260*, 1124–1127.
[6] a) M. Domenech, I. Marrero-Berrios, M. Torres-Lugo, C. Rinaldi, *ACS Nano* **2013**, *7*, 5091–5101; b) D. H. Kim, E. A. Rozhkova, I. V. Ulasov, S. D. Bader, T. Rajh, M. S. Lesniak, V. Novosad, *Nat. Mater.* **2010**, *9*, 165–171; c) R. J. Mannix, S. Kumar, F. Cassiola, M. Montoya-Zavala, E. Feinstein, M. Prentiss, D. E. Ingber, *Nat. Nanotechnol.* **2008**, *3*, 36–40; d) M. H. Cho, E. J. Lee, M. Son, J. H. Lee, D. Yoo, J. W. Kim, S. W. Park, J. S. Shin, J. Cheon, *Nat. Mater.* **2012**, *11*, 1038–1043.
[7] C. Hoffmann, E. Mazari, S. Lallet, R. Le Borgne, V. Marchi, C. Gosse, Z. Gueroui, *Nat. Nanotechnol.* **2013**, *8*, 199–205.
[8] H. Ebrahimian, M. Giesguth, K. J. Dietz, G. Reiss, S. Herth, *Appl. Phys. Lett.* **2014**, *104*, 063701.
[9] L. J. Eggermont, L. E. Paulis, J. Tel, C. G. Figdor, *Trends Biotechnol.* **2014**, *32*, 456–465.
[10] a) J. Yan, S. C. Bae, S. Granick, *Adv. Mater.* **2015**, *27*, 874–879; b) R. M. Erb, N. J. Jenness, R. L. Clark, B. B. Yellen, *Adv. Mater.* **2009**, *21*, 4825–4829; c) A. Ruditskiy, B. Ren, I. Kretschmar, *Soft Matter* **2013**, *9*, 9174–9181.
[11] S. K. Smoukov, S. Gangwal, M. Marquez, O. D. Velev, *Soft Matter* **2009**, *5*, 1285–1292.
[12] a) R. S. Lewis, *Annu. Rev. Immunol.* **2001**, *19*, 497–521; b) S. Feske, *Nat. Rev. Immunol.* **2007**, *7*, 690–702.
[13] B. Chen, Y. L. Jia, Y. Gao, L. Sanchez, S. M. Anthony, Y. Yu, *ACS Appl. Mater. Interfaces* **2014**, *6*, 18435–18439.
[14] a) D. Delcassian, D. Depoil, D. Rudnicka, M. Liu, D. M. Davis, M. L. Dustin, I. E. Dunlop, *Nano Lett.* **2013**, *13*, 5608–5614; b) D. T. Kim, J. B. Rothbard, D. D. Bloom, C. G. Fathman, *J. Immunol.* **1996**, *156*, 2737–2742.

Received: February 2, 2016

Revised: March 20, 2016

Published online: May 4, 2016